Melittin-Induced Bilayer Leakage Depends on Lipid Material Properties: Evidence for Toroidal Pores

Daniel Allende,*† S. A. Simon,† and Thomas J. McIntosh*
Departments of *Cell Biology and †Neurobiology, Duke University Medical Center, Durham, North Carolina 27710

ABSTRACT The membrane-lytic peptide melittin has previously been shown to form pores in lipid bilayers that have been described in terms of two different structural models. In the "barrel stave" model the bilayer remains more or less flat, with the peptides penetrating across the bilayer hydrocarbon region and aggregating to form a pore, whereas in the "toroidal pore" melittin induces defects in the bilayer such that the bilayer bends sharply inward to form a pore lined by both peptides and lipid headgroups. Here we test these models by measuring both the free energy of melittin transfer (ΔG°) and melittin-induced leakage as a function of bilayer elastic (material) properties that determine the energetics of bilayer bending, including the area compressibility modulus (K_a), bilayer bending modulus (k_c), and monolayer spontaneous curvature (R_o). The addition of cholesterol to phosphatidylcholine (PC) bilayers, which increases K_a and k_c, decreases both ΔG° and the melittin-induced vesicle leakage. In contrast, the addition to PC bilayers of molecules with either positive R_o, such as lysoPC, or negative R_o, such as dioleoylglycerol, has little effect on ΔG°, but produces large changes in melittin-induced leakage, from 86% for 8:2 PC/lysoPC to 18% for 8:2 PC/dioleoylglycerol. We observe linear relationships between melittin-induced leakage and both K_a and $1/R_o^2$. However, in contrast to what would be expected for a barrel stave model, there is no correlation between observed leakage and bilayer hydrocarbon thickness. All of these results demonstrate the importance of bilayer material properties on melittin-induced leakage and indicate that the melittin-induced pores are defects in the bilayer lined in part by lipid molecules.

INTRODUCTION

The lipid bilayer environment affects the characteristics of several types of channels, including membrane protein channels, such as sodium channels (Lundbaek et al., 2004), stretch-activated potassium channels (Maingret et al., 2000; Patel et al., 2001), and voltage-gated potassium channels (Oliver et al., 2004), as well as channels or pores formed by small peptides such as gramicidin (Lundbaek and Andersen, 1994), alamethicin (Keller et al., 1993) and cathelicidin (Basanez et al., 2002). One of the most commonly studied pore-forming peptides is melittin from the venom of certain honeybees (Gauldie et al., 1976). Melittin disrupts the barrier function of cell membranes (Banemann et al., 1998; Dempsey, 1990; Epand and Vogel, 1999) and forms channels in planar bilayers (Pawlak et al., 1991; Tosteson and Tosteson, 1981; Stankowski et al., 1991). In terms of lipid vesicles, strong evidence for pore formation, rather than bilayer dissolution, has been obtained from experiments showing that small, but not large, water-soluble fluorescent probes leak from the interior of vesicles incubated with melittin (Ladokhin et al., 1997a; Matsuzaki et al., 1997; Rex, 1996; Yang et al., 2001).

There have been several studies designed to determine the architecture of the pores induced by melittin (Ladokhin et al., 1997a; Matsuzaki et al., 1997; Takei et al., 1999; Yang et al., 2001) and other cell-lytic peptides, such as the antimicrobial peptides magainin (Ludtke et al., 1996; Matsuzaki et al., 1996, 1998; Yang et al., 2000) and cathelicidin (Basanez et al., 2002). Two general classes of peptide-induced pores have often been described. In both models, the peptide is oriented perpendicular to the plane of the host bilayer, consistent with oriented circular dichroism data for melittin (Yang et al., 2001) and the observation that melittin translocates across the bilayer after disintegration of the pore (Matsuzaki et al., 1997). However, the role of the lipid molecules is quite different in the two models. In the ''barrel stave'' model, the peptides span a nearly flat bilayer and aggregate to line an aqueous channel, whereas in the other general class of peptide-induced pore, typified by the ''toroidal pore'' model (Ludtke et al., 1996; Matsuzaki et al., 1998; Yang et al., 2001; Zemel et al., 2003), the lipid bilayer sharply bends so that the lipid headgroups form part of the lining of the pore (Fig. 1 *A*). The antimicrobial peptide alamethicin has been shown to be an example of the barrel stave pore (Barranger-Mathys and Cafiso, 1996; Kessel et al., 2000; Zemel et al., 2003), whereas magainin (Ludtke et al., 1996; Matsuzaki et al., 1998), the magainin analog MSI-78 (Hallock et al., 2003), and cathelicidin (Basanez et al., 2002; Henzler Wildman et al., 2003) are thought to induce toroidal pores. However, in the case of melittin, both barrel stave (Ladokhin and White, 2001; Rex and Schwarz, 1998) and toroidal models (Yang et al., 2001) have been invoked.

Since in the toroidal pore model the lipids must sharply bend to line the pore (Fig. 1 *A*), the peptide-induced leakage should critically depend on bilayer mechanical or material properties, especially those involving bending. Indeed, Matsuzaki et al. (1998) and Basanez et al. (2002) showed that the bilayer curvature properties do modify the dye

Submitted July 15, 2004, and accepted for publication November 30, 2004.

Address reprint requrests to Thomas J. McIntosh, E-Mail: t.mcintosh@cellbio.duke.edu.

0006-3495/05/03/1828/10 $2.00

doi: 10.1529/biophysj.104.049817

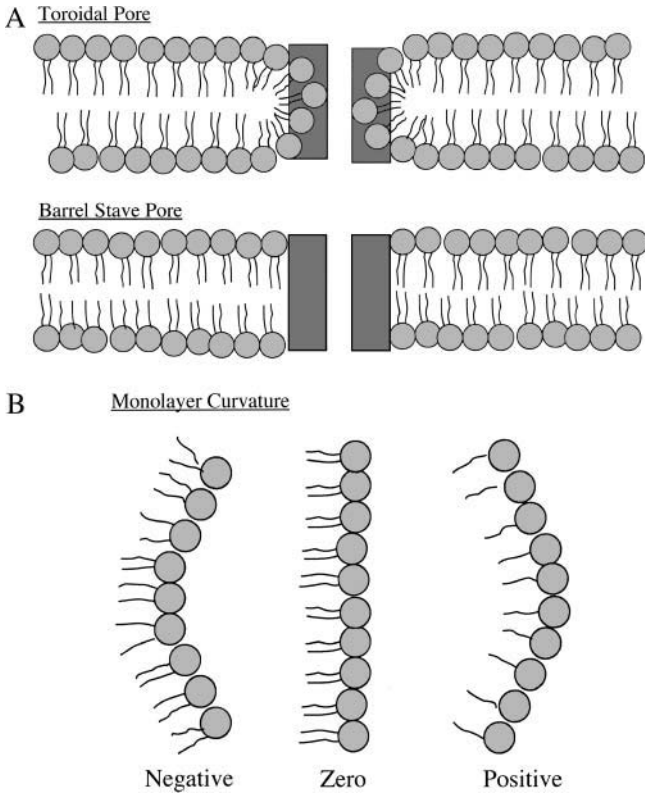

FIGURE 1 Schematic drawings of sections through (*A*) ''toroidal pore'' and ''barrel stave pore'' models and (*B*) models for monolayer spontaneous curvature. In *A*, peptides are depicted as rectangular dark shaded boxes, and lipids are shown with circular light shaded headgroups and wavy hydrocarbon chains. In *B*, lipids that have approximately the same excluded area in their headgroup and acyl chain regions (EPC or SOPC) form structures with near zero membrane curvature (*middle image*), lipids whose excluded headgroup area is smaller than the area of its acyl chains (DOPC, DOPE, or DOG) form structures with negative curvature (*image on left*), whereas lipids whose headgroup area is larger than its acyl chain area (lysoPC) have positive curvature (*image on right*).

leakage induced by magainin 2 and hagfish cathelicidin, respectively, providing strong evidence that these peptides form toroidal pores. However, for melittin, quantitative relationships have not been obtained between dye leakage and bilayer material properties.

Theoretical treatments (Chen and Rand, 1997; Lundbaek et al., 2003; Nielsen et al., 1998; Nielsen and Andersen, 2000) show that bilayer bending or deformation depends on bilayer mechanical properties, including the isothermal area compressibility modulus (K_a), the bending modulus (k_c), and the monolayer spontaneous radius of curvature (R_o). Specifically, the energy of bilayer deformation contains terms involving changes in the bilayer's area and curvature that are proportional to K_a and k_c/R_o^2, respectively (Huang, 1986; Lundbaek et al., 2003). K_a is a measure of the cohesion between lipid molecules in the plane of the bilayer, k_c is a measure of the elastic bending of the bilayer, and R_o relates to the equilibrium curvature or tendency of the lipid molecules to form curved structures (Fig. 1 *B*). Each of these parameters are functions of the bilayer composition, as both K_a and k_c depend on bilayer hydrocarbon chain composition and cholesterol content (Evans and Needham, 1987; Needham, 1995; Needham and Nunn, 1990; Rawicz et al., 2000) and R_o depends on lipid headgroup type and hydrocarbon chain composition (Fuller and Rand, 2001; Leikin et al., 1996; Rand et al., 1990; Szule et al., 2002). In the case of transmembrane peptides or proteins (such as occur in the barrel stave model), the bilayer deformation energy will also depend on the thickness of the bilayer hydrocarbon region (Dan and Safran, 1998; Lundbaek et al., 2003; May and Ben-Shaul, 1999; Nielsen et al., 1998; Nielsen and Andersen, 2000) due to the energetic cost of hydrophobic mismatch between the transmembrane length of the peptide and the thickness of the bilayer hydrocarbon core (d_{hc}).

For either class of pore formation (Fig. 1 *A*), the peptide-induced leakage is a function of the amount of peptide bound to the membrane, often characterized by the free energy of partitioning to the bilayer (ΔG^o). Therefore, analysis of melittin-induced leakage must consider ΔG^o, which is also expected to depend on the material properties of the bilayer. In this regard, the partitioning of water soluble peptides into lipid bilayers involves several contributions to the free energy (Ben-Tal et al., 1996a; Kessel et al., 2000; Kessel and Ben-Tal, 2002; Mouritsen and Bloom, 1984; White and Wimley, 1999), including terms due to electrostatic interactions, conformational changes in the peptide upon binding, the hydrophobic effect, and ''bilayer effects'' due in part to the peptide interfering with conformational freedom of the lipid hydrocarbon chains and causing changes in lipid area/molecule. Indeed several studies have shown that bilayer effects can provide an appreciable contribution to ΔG^o (Ben-Shaul et al., 1996; Ben-Tal et al., 1996a,b; Kessel et al., 2000; White and Wimley, 1999). Moreover, in the case of melittin we have shown that the magnitude of ΔG^o decreases linearly with increasing K_a, indicating that increases in cohesive energy oppose the penetration of exogenous compounds into the bilayer (Allende and McIntosh, 2003; Allende et al., 2003). That is, incorporation of a peptide into the bilayer requires the separation of adjacent lipid molecules, which is opposed by increases in K_a.

In this article, we determine how structural and material properties of the bilayer modulate both ΔG^o and melittin-induced leakage. Our goal is to obtain quantitative relationships between both binding and leakage and the parameters K_a, k_c, R_o, and d_{hc} by systematically changing the bilayer composition. Such data should provide insights on the organization of melittin-induced pores. Specifically, to separate bilayer effects on melittin binding from subsequent events in melittin-induced pore formation, we compare bilayer systems with similar amounts of bound melittin (similar values of ΔG^o). This is accomplished by measuring the free energy of melittin binding ($\Delta G°$) and melittin-induced vesicle leakage for phospholipid bilayers as a function of

hydrocarbon chain composition, headgroup type, and cholesterol concentration.

MATERIALS AND METHODS

Materials

Egg phosphatidylcholine (EPC), 1-stearoyl-2-oleoyl-*sn*-glycero-3-phosphocholine (C18:0/C18:1PC or SOPC), 1,2-dioleoyl-*sn*-glycero-3-phosphocholine (diC18:1PC or DOPC), 1,2-dilinoleoyl-*sn*-glycero-3-phosphocholine (diC18:2PC or DLinPC), 1,2-dioleoyl-*sn*-glycero-3-phosphoethanolamine (diC18:1PE or DOPE), bovine brain phosphatidylserine sodium salt (PS), bovine brain sphingomyelin (SM), dioleoylglycerol (DOG), and cholesterol (Ch) were purchased from Avanti Polar Lipids (Alabaster, AL). *N*-myristoyl-sphingosine-1-succinyl(methoxy (polyethylene glycol))-2000 (PEG-Cer) was purchased from Northern Lipids (Vancouver, Canada). Monooleoylphosphatidylcholine (lysoPC), Hepes, sulforhodamine B (SRB) and melittin (GIGAVLKVLTTGLPALISWIKRKRQQ; 93% minimum purity) were purchased from Sigma Chemical (St. Louis, MO). All compounds were used without further purification.

Peptide binding measurements

Peptide binding experiments were performed with large unilamellar vesicles (LUVs) following procedures detailed in Allende and McIntosh (2003). In brief, LUVs were made by codissolving the lipids in chloroform, removing the solvent by rotary evaporation, forming a multilamellar vesicle suspension in 5 mM Hepes, 25 mM KCl, pH 7.4 with extensive vortexing with 5 freeze-thaw cycles, and then extruding the suspension 20 times through two stacked 0.1-μm polycarbonate filters in a LiposoFast lipid extruder (Northern Lipids). After extrusion, the phospholipid concentrations in the LUVs were determined by phosphate analysis (Chen et al., 1956).

The binding of melittin to LUVs was measured with an ultrafiltration assay (Sophianopoulos et al., 1978) that separated lipid and lipid/peptide complexes from free peptide with Centricon-10 filters (Millipore, Bedford, MA). Melittin was added to LUVs and incubated for 30 min before a 1-h centrifugation at 6,000 $\times$ *g* through the filter (Voglino et al., 1998, 1999). Melittin was used at 10 μM concentration, where it is in a monomeric form (Faucon et al., 1979; Quay and Condie, 1983). All experiments were performed at 20°C in the bilayer's liquid-crystalline phase. The free melittin concentration was determined by comparing the measured tryptophan fluorescence in the eluate to the fluorescence intensity of melittin standards. The fluorescence intensities were measured at an emission wavelength of 356 nm in a Jobin Yvon (Edison, NJ) SPEX fluorometer DM-3000. The amount of melittin bound to the lipid was determined by subtracting the free peptide concentration from the total peptide concentration.

The molar partition coefficient (K_p) was calculated from binding measurements as described previously (Allende and McIntosh, 2003). Under conditions where the molar concentration of peptide in the bilayer is much smaller than the molar concentration of lipid, K_p can be written as

$$K_p = (P_{bil}W)/(P_{wat}L), \quad (1)$$

where P_{bil} and P_{wat} are the bulk molar concentrations of peptide in the bilayer and water phases, respectively, and L and W are the molar concentrations of lipid and water, respectively (Ladokhin et al., 1997b). For LUVs, the outer monolayer of the bilayer contains ~50% of the total lipid, so L was taken to be 50% of the total lipid concentration (Allende and McIntosh, 2003). The free energy of transfer was calculated from

$$\Delta G^\circ = -RT\ln(K_p), \quad (2)$$

where R is the molar gas constant and T is the temperature in degrees Kelvin.

Melittin-induced leakage

The leakage induced by melittin was measured at 20°C by recording the release of vesicle-encapsulated SRB following published procedures (Benachir et al., 1997; Rex et al., 2002). LUVs loaded with SRB were prepared as described above except that the Hepes buffer contained a self-quenching concentration (70 mM) of SRB, resulting in a liposome dispersion with low background fluorescence intensity (I_B) measured with excitation and emission wavelengths of 560 and 590 nm, respectively. Free SRB surrounding the LUVs was removed by size exclusion chromatography using a column filled with Sephadex G-50 (Pharmacia Biotech, Uppsala, Sweden). The fraction loaded with SRB that eluted from the column was diluted with isosmotic buffer (5 mM Hepes, 130 mM KCl, pH 7.4) to obtain a lipid concentration of 1–6 μM. The addition of melittin (at a lipid/peptide ratio of 200:1 for all experiments) caused the release of SRB to the medium. SRB leakage was monitored by measuring the increase in fluorescence intensity (I_F). After 5 min, Triton X-100 (0.1 vol%) was added to obtain a 100% SRB leakage value (I_T). The percentage of SRB release was calculated according to

$$\%\,\text{Release} = (I_F - I_B)/(I_T - I_B)\times 100\%. \quad (3)$$

For all fluorescence experiments, the samples were continually mixed with a small stirring bar. All leakage experiments were performed at least three times, with the maximum observed SRB release varying by <5%.

The average leakage time course curves were fit using Sigma Plot with the relationship

$$\%\,\text{Release} = L_{max}(1 - \exp(-t/\tau)), \quad (4)$$

where L_{max} represents the maximum (steady-state) leakage, t is the time after the addition of melittin, and (tau) is the time constant.

X-ray diffraction

X-ray diffraction analysis for bilayers of 8:2 EPC/DOG and 1:1 DOPC/DOPE was performed as described in detail previously (Gandhavadi et al., 2002; McIntosh and Holloway, 1987; McIntosh et al., 1987, 1989). In brief, oriented lipid multilayers were prepared by placing a drop of an aqueous suspension of multilamellar vesicles onto a curved glass substrate and then drying under a gentle stream of nitrogen. The multilayers on the glass substrate were mounted in a constant humidity sample chamber on a line-focus (single mirror) x-ray camera. Relative humidities in the range of 98%–86% were set by incubation with saturated salt solutions. X-ray patterns were recorded at ambient temperature on Kodak (Rochester, NY) DEF-5 x-ray film.

To obtain electron density profiles across the bilayer, a Fourier analysis of the x-ray diffraction patterns was performed (McIntosh and Holloway, 1987; McIntosh et al., 1987). Integrated intensities were obtained for each diffraction order by measuring the area under each diffraction peak, and structure amplitudes were obtained by applying standard correction factors for oriented specimens (McIntosh et al., 1987). Since the diffraction patterns had very similar repeat periods and intensity distributions as multilayers of EPC (McIntosh and Simon, 1986; McIntosh et al., 1987), we used the same phase angles as we had determined previously for EPC (McIntosh and Simon, 1986; McIntosh et al., 1987).

RESULTS

We measured the free energy of melittin transfer and melittin-induced leakage for several bilayer systems that varied in their elastic and structural properties. In particular, as shown in Table 1, we examined bilayers as a function of area compressibility modulus (K_a), bilayer bending modulus (k_c), spontaneous radius of curvature (R_o), and hydrocarbon thickness

TABLE 1 Binding and leakage data for melittin with LUVs

Lipid	ΔG° (kcal/mol)	L_{max} (%)	τ (s)	K_a (dyn/cm)	k_c (10^{-19} J)	$1/R_o$ (1/Å)	d_{hc} (Å)
EPC	−7.6 ± 0.1	73	13	171	—	~0	27.8
SOPC	−7.8 ± 0.1	73	20	235	0.90	~0	30.7
DOPC	−7.6 ± 0.2	56	48	265	0.85	−0.011	26.9
DLinPC	−7.6 ± 0.2	59	32	247	0.44	—	24.9
EPC/Ch (1:1)	−6.4 ± 0.2	3	—	(660)	(2.46)	—	—
SOPC/Ch (1:1)	−6.1 ± 0.1	3	—	660	2.46	—	—
EPC/PS/Ch (35:15:50)	−7.8 ± 0.3	8	238	(660)	(2.46)	—	—
SM/Ch (1:1)	−4.5 ± 1.0	1	—	1725	5.40	—	—
DOPC/DOPE (8:2)	−7.7 ± 0.1	34	51	—	(0.9)	−0.016	—
DOPC/DOPE (1:1)	−7.8 ± 0.1	23	130	—	(0.9)	−0.023	27.3
EPC/LysoPC (8:2)	−8.1 ± 0.2	86	2	90	—	0.005	26.9
EPC/DOG (8:2)	−7.3 ± 0.1	18	135	—	—	−0.020	27.7
EPC/PEG-Cer (85:15)	−7.9 ± 0.1	11	10	—	—	—	—

Compressibility moduli (K_a) and bending moduli (k_c) are taken from Needham and Nunn (1990), Zhelev (1998), and Rawicz et al. (2000) with the values of k_c for 8:2 DOPC/DOPE and 1:1 DOPC/DOPE estimated based on measurements for DOPC (Rawicz et al., 2000) and 1:3 DOPC/DOPE (Rand et al., 1990). Values in parentheses for EPC/cholesterol and EPC/PS/cholesterol are the values for SOPC/cholesterol (see text for details). Spontaneous curvature data ($1/R_o$) are taken from Rand et al. (1990), Leikin et al. (1996), Chen and Rand (1997), Fuller and Rand (2001), and Szule et al. (2002). Bilayer hydrocarbon thicknesses (d_{hc}) are taken from Fig. 5 and from McIntosh and Simon (1986), McIntosh et al. (1995), and Rawicz et al. (2000).

(d_{hc}). Results of typical leakage experiments for EPC, 8:2 EPC/lysoPC, and 8:2 EPC/DOG are shown in Fig. 2.

Effect of compressibility modulus on melittin binding and leakage

Cholesterol decreases the area per phospholipid molecule and thereby increases bilayer in-plane cohesive interactions. This cohesive interaction is reflected in the magnitude of K_a, which increases significantly with increasing cholesterol concentration (Needham and Nunn, 1990). The addition of equimolar cholesterol into EPC or SOPC and SM decreased both ΔG° and decreased melittin-induced leakage (Table 1); ΔG° decreased from −7.8 kcal/mol for SOPC to −6.1 kcal/mol for 1:1 SOPC/cholesterol and the steady-state leakage decreased from 73% for SOPC to 3% for SOPC/cholesterol. Similar results were obtained for EPC and EPC/cholesterol (Table 1). Equimolar SM/cholesterol, which has an extremely large K_a (Needham and Nunn, 1990), gave the lowest value of both ΔG° and leakage (Table 1). For electrically neutral bilayers containing equimolar cholesterol (SOPC/cholesterol, EPC/cholesterol, or SM/cholesterol), the leakage levels were so low that accurate time constants τ could not be obtained by fitting the leakage curves to Eq. 4.

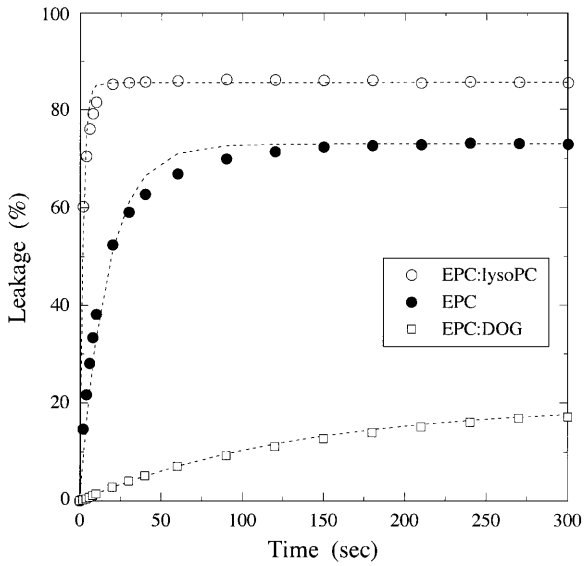

FIGURE 2 Typical leakage curves for bilayers of EPC (○), 8:2 EPC/lysoPC (●), and 8:2 EPC/DOG (□). The addition of melittin at time $t = 0$ caused a rapid leakage of encapsulated SRB for the first minute or two, after which the leakage leveled off to a nearly constant value. For each lipid system, the dotted lines represent fits ($R^2 > 0.99$) using Eq. 4, % Release $= L_{max}(1 - e^{-t/\tau})$.

It might be argued that the low leakage level of cholesterol-containing bilayers was due solely to the low binding. Therefore, to increase the binding of melittin of cholesterol-containing bilayers to that of EPC, we added negatively charged PS to EPC/cholesterol bilayers. Thus, ΔG° was −7.8 kcal/mol for LUVs composed of EPC/PS/cholesterol (35:15:50), which is similar to the value for EPC or SOPC bilayers (Table 1); however, the extent of SRB release was only 8% for EPC/PS/cholesterol (Table 1), which was much lower than the SRB release of 54% from EPC/PS vesicles (Allende and McIntosh, 2003). In addition, for EPC/PS/cholesterol (35:15:50) bilayers, the SRB release was characterized by a time constant of 238 s, which was quite slow compared to $\tau = 13$ s for EPC bilayers (Table 1).

Fig. 3 shows that the SRB leakage from bilayers with similar amounts of bound melittin (ΔG^o between −7.6 kcal/mol and −7.8 kcal/mol) decreased linearly with increasing K_a, and τ increased linearly with increasing K_a. These results indicate that the increased bilayer cohesiveness caused by the addition of cholesterol modified melittin-induced leakage.

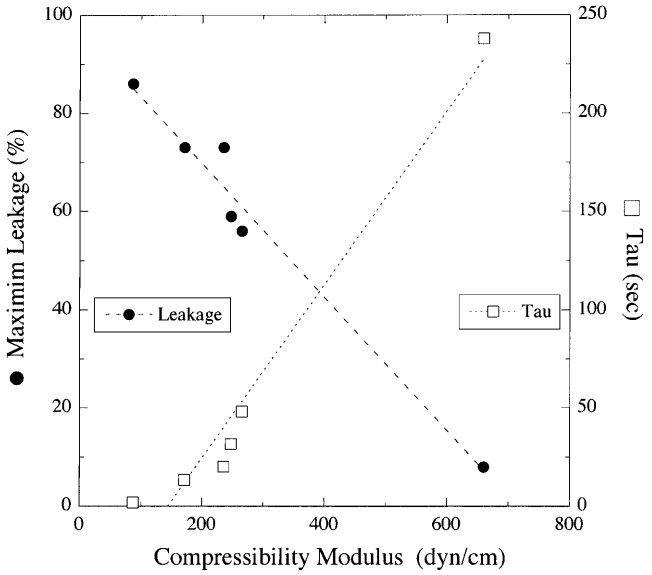

FIGURE 3 Plot of melittin-induced leakage (L_{max}, ●) and time constant (τ, □) versus area compressibility modulus (K_a) for EPC/lysoPC, EPC, SOPC, DOPC, DLinPC, and EPC/PS/cholesterol (35:15:50). Dashed and dotted lines represent least-square linear fits to the plots of L_{max} versus K_a ($R^2 = 0.97$) and τ versus K_a ($R^2 = 0.96$), respectively.

Effect of bending modulus on melittin binding and leakage

The bilayer bending modulus is also increased by the addition of cholesterol (Table 1), so that experiments with cholesterol-containing bilayers do not distinguish between effects of K_a and k_c. However, it has recently been shown that K_a and k_c have different dependencies on the number of double bonds in the phospholipid hydrocarbon chains (Rawicz et al., 2000). That is, although K_a is nearly the same for SOPC, DOPC, and DLinPC, k_c is smaller by a factor of 2 for DLinPC compared to SOPC or DOPC (Table 1). Therefore, melittin-binding experiments with bilayers containing varying numbers of double bonds should allow us to separate the effects of K_a and k_c. We found that melittin partitioning was similar for lipids with 1, 2, or 4 double bonds per molecule; $\Delta G°$ was −7.8 kcal/mol for SOPC and −7.6 kcal/mol for DOPC and DLinPC bilayers. Interestingly, the leakage (L_{max}) was somewhat lower for DOPC and DLinPC compared to SOPC (Table 1).

Effect of intrinsic membrane curvature on melittin binding and leakage

We next examined the effects on melittin binding and melittin-induced leakage of lipids with a range of spontaneous curvature values produced by changes in headgroup and hydrocarbon chain compositions (Fig. 1 *B*). The values of $1/R_o$ shown in Table 1 were taken from experimental measurements of Rand et al. (1990), Fuller and Rand (2001), and Szule et al. (2002). All of these lipid systems, which are electrically neutral, gave similar values of $\Delta G°$ (between −7.3 kcal/mol and −8.1 kcal/mol). However, as shown in Fig. 2, melittin-induced leakage was dramatically changed by the addition to EPC of molecules with different spontaneous curvatures. The melittin-induced leakage varied from a maximum of 86% for 1:1 EPC/lysoPC to low values of 23% for 1:1 DOPC/DOPE and 18% for 8:2 EPC/DOG. In a similar experiment with magainin 2 in phosphatidylglycerol bilayers, Matsuzaki et al. (1998) observed an increase in leakage with the addition of lysoPC and a decrease with the incorporation of PE. In addition, the time constants (τ) were also modified by changes in $1/R_o$ (Table 1). Comparisons of all of the data in Table 1 showed that there was linear dependence with $1/R_o^2$ for both melittin-induced leakage and τ (Fig. 4).

Effect of PEG2000-ceramide on melittin binding and leakage

For these experiments, we used EPC bilayers containing 15% PEG2000-Cer. Under these conditions, the PEG polymer forms a brush conformation at the liposome surface (deGennes, 1987; Kenworthy et al., 1995a, 1995b). Because PEG2000-ceramide has a very large headgroup, it might be expected to exhibit a positive curvature and, thus, facilitate leakage in a similar manner to lysoPC. However, in agreement with previous studies (Rex et al., 2002), the addition of

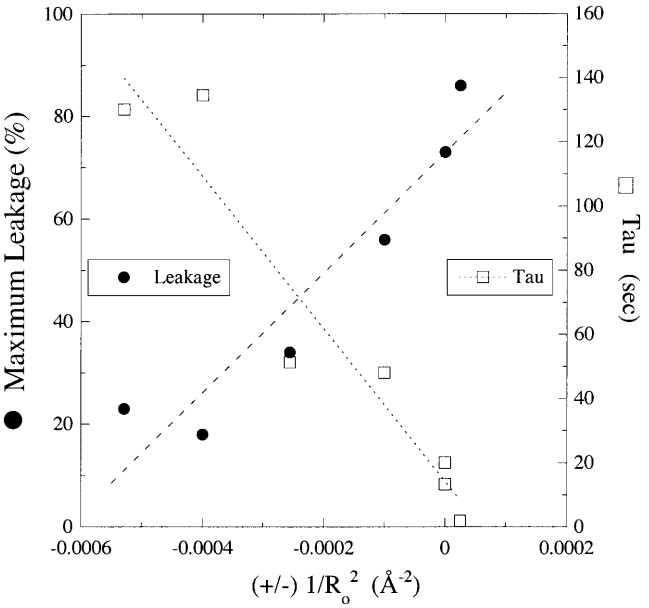

FIGURE 4 Plot of melittin-induced leakage (L_{max}, ●) and time constant (τ, □) versus (±) $1/R_o^2$ for SOPC, DOPC, 1:1 DOPC/DOPE, 8:2 DOPC/DOPE, 8:2 EPC/lysoPC, and 8:2 EPC/DOG. The signs on the abscissa are present because we have defined the curvature elastic energy as positive for bilayers with positive curvature (8:2 EPC/lysoPC) and negative for bilayers with negative curvature (8:2 EPC/DOG). Dashed and dotted lines are least-square linear fits to the plots of L_{max} versus $1/R_o^2$ ($R^2 = 0.90$) and τ versus $1/R_o^2$ ($R^2 = 0.92$), respectively.

PEG2000-Cer to EPC bilayers reduced the melittin-induced leakage from 73% to 11% and yet had no appreciable effect on melittin binding (Table 1).

Effect of hydrocarbon thickness on melittin binding and leakage

We next investigated how changes in bilayer hydrocarbon thickness (d_{hc}) modify melittin-induced leakage. Electron density profiles have been published for EPC (McIntosh and Simon, 1986; McIntosh et al., 1987), EPC/lyso PC (McIntosh et al., 1995), DOPC, DLinPC, and SOPC (Rawicz et al., 2000). Here we determined electron density profiles at comparable resolution for 8:2 EPC/DOG and 1:1 DOPC/DOPE. For both 8:2 EPC/DOG and 1:1 DOPC/DOPE, four orders of a lamellar repeat period were obtained for 86%, 93%, and 98% relative humidity. The repeat periods and intensity distributions were similar for these patterns to those previously recorded patterns for EPC under the same conditions (McIntosh et al., 1987), so we used the same phase angles that were obtained for EPC. The resulting electron density profiles are shown in Fig. 5, along with the comparable profile for EPC. For each profile, the center of the bilayer is located at the origin; the low electron density trough in the center of the profile corresponds to the terminal methyl groups at the ends of the hydrocarbon chains; the medium density regions on either side of this trough correspond to the methylene chain regions of the bilayer; and the high electron density peaks near the edge of the profile correspond to the lipid headgroups. Vertical dotted lines are drawn through the headgroup peaks of EPC and show that the headgroup-to-headgroup distance (d_{pp}) thickness across the bilayer was quite similar for each system shown in Fig. 5.

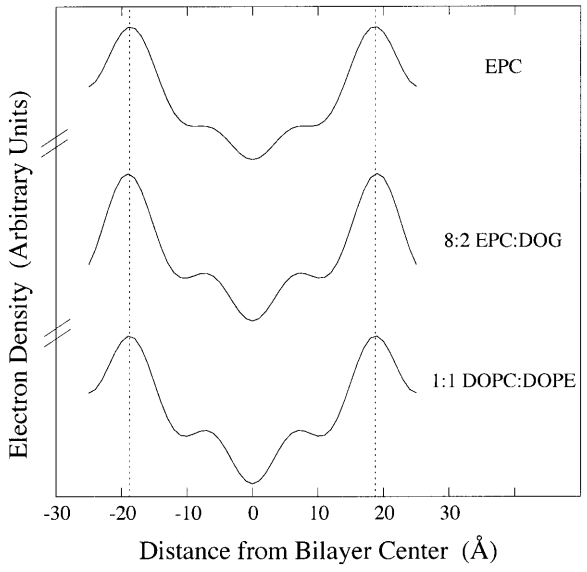

FIGURE 5 Electron density profiles of EPC, 8:2 EPC/DOG, and 1:1 DOPC/DOPE. The profile for EPC was taken from McIntosh et al. (1987).

Values of d_{pp} were 37.7 Å ± 0.6 Å (mean ± SD) for 8:2 EPC/DOG and 37.3 Å ± 0.8 Å for 1:1 DOPC/DOPE. Since the distance between the center of each headgroup peak and the edge of the bilayer hydrocarbon region is ~5 Å (McIntosh and Simon, 1986; McIntosh et al., 1987), the values of bilayer hydrocarbon thickness shown in Table 1 were calculated from $d_{hc} = d_{pp} - 10$ Å.

Fig. 6 shows a plot of observed leakage and time constants versus bilayer hydrocarbon thickness for bilayers with very similar values of ΔG^o (Table 1). It can be seen that there is no obvious correlation between either L_{max} or τ with hydrocarbon thickness for the range of d_{hc} from 24.9 Å to 30.7 Å. Moreover, for bilayers with similar hydrocarbon thickness (26.9 Å–27.8 Å), L_{max} ranged from 18% to 86%, and τ ranged from 2 to 135 s (Fig. 6).

DISCUSSION

The data presented in this article show that both the free energy of partitioning and melittin-induced leakage depend critically on the bilayer's composition and material properties. The primary goal of this study is to distinguish between different models (Fig. 1 *A*) for melittin-induced pore formation by analyzing leakage as a function of bilayer structural and material properties. For a given lipid concentration, it has previously been found that the melittin-induced bilayer leakage increases in a sigmoidal manner with increasing peptide concentration in the aqueous phase (Benachir and Lafleur, 1995; Benachir et al., 1997; Hincha and Crowe, 1996; Rex et al., 2002). Different bilayer types exhibit a range of sensitivities that depend on a variety of factors, including the presence of fixed charges or cholesterol in the

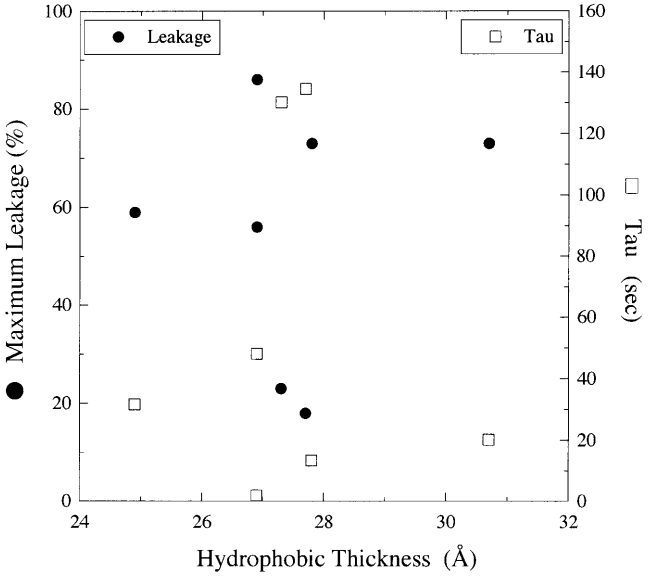

FIGURE 6 Plot of melittin-induced leakage (L_{max}, ●) and time constant (τ, □) versus bilayer hydrocarbon thickness (d_{hc}) for EPC, SOPC, DOPC, 8:2 DOPC/DOPE, 1:1 DOPC/DOPE, 8:2 EPC/DOG, and 8:2 EPC/LysoPC.

bilayer (Benachir et al., 1997; Hincha and Crowe, 1996). Since the melittin-induced leakage can depend on the amount of melittin bound (Benachir et al., 1997), we compared leakage data from systems with similar amounts of bound peptide (Table 1). For these systems, the effects of melittin cannot be attributed to different concentrations of peptide in the bilayer but, rather, must be due to the role the bilayer plays in subsequent steps in melittin-induced pore formation. As done by Hincha and Crowe (1996), for EPC we chose a melittin concentration near the middle of the sigmoidal region of the leakage-concentration curve so that we could observe either increases or decreases in leakage with changes in bilayer composition (Table 1). An implicit assumption in the quantitative aspect of our analysis was that the observed leakages for different bilayer compositions were not near either extreme of their sigmoidal leakage-concentration relationships.

Throughout this article we characterized the melittin-induced leakage with the parameters L_{max} and τ (Eq. 4). The data presented in Table 1 show that there was a correlation between L_{max} and τ in that τ monotonically decreased with increasing L_{max}. The physical meaning of each parameter is model dependent, involving assumptions about the formation and dissolution of the pores, the rate limiting step of pore formation at zero applied voltage, and the homogeneity of the melittin distribution. Nevertheless, L_{max} is related to the number of open channels and the channel conductance, and τ is related to the rate of channel formation. Thus, the observation that the incorporation of lysoPC into EPC bilayers increased L_{max} and decreased τ implies that lysoPC increased the number of open channels and/or their conductance and increased the rate of channel formation. The incorporation of DOG into EPC bilayers had the opposite effects. In this article, we do not attempt to formulate a kinetic model of melittin-induced leakage, but are primarily interested in determining how bilayer properties affect this leakage. Thus, the observed correlations between the material properties of the bilayer and either L_{max} or τ (Figs. 3 and 4) suffice to show the role of bilayer material properties in melittin-induced pore formation.

Area compressibility modulus and bilayer bending modulus

As seen in Table 1, both K_a and k_c were markedly increased by the introduction of cholesterol into PC bilayers. Previous work has shown that both melittin binding (Allende and McIntosh, 2003; Allende et al., 2003; Benachir et al., 1997) and melittin-induced leakage (Allende and McIntosh, 2003; Benachir et al., 1997) decrease with increasing concentration of cholesterol in PC vesicles. Therefore, the reduced leakage caused by the presence of cholesterol could simply be due to a lower amount of melittin present in the bilayer, rather than to an effect of K_a or k_c on pore formation. To test that possibility, we added the negatively charged lipid PS to EPC/cholesterol bilayers to increase melittin binding to that of EPC bilayers. For bilayers with similar melittin binding (ΔG^o between -7.6 and -7.8 kcal/mol), melittin-induced leakage sharply decreased with increasing K_a (Fig. 3). This implies that the material properties of the bilayer, as measured by K_a or k_c, play an important role in melittin-induced pore formation, as well as in melittin partitioning. An assumption in Fig. 3 is that K_a is the same for 1:1 EPC/cholesterol and 35:15:50 EPC/PS/cholesterol. That is, we assume that PS and EPC have similar values of K_a. This appears to be a reasonable assumption, in that addition of 30 mol % PS does not appreciably change K_a for SOPC bilayers (Evan Evans, University of British Columbia, personal communication, 2004).

It is difficult to experimentally separate the effects of K_a and k_c on melittin-induced pore formation, since for most bilayer systems these parameters are related by $k_c \sim (d_{hc})^2 \times K_a$ (Rawicz et al., 2000). However, phospholipids with polyunsaturated hydrocarbon chains (such as DLinPC) are more bendable than bilayers containing monounsaturated hydrocarbon chains (DOPC; Rawicz et al., 2000). Thus, as shown in Table 1, although DOPC and DLinPC have similar values of K_a, the measured value of k_c is significantly smaller for DLinPC (Rawicz et al., 2000). Since the melittin-induced leakage was similar for DOPC and DLinPC, this implies that values of k_c by themselves are not good predictors of bilayer susceptibility peptides. In agreement with theoretical treatments (Huang, 1986; Lundbaek et al., 2003) indicating that the energy of bilayer bending depends on k_c/R_o^2, our data point to an additional factor involved in bilayer bending, namely the spontaneous curvature (R_o).

Spontaneous curvature

As shown in Fig. 4, for bilayers with similar values of ΔG^o, there is a linear relationship between melittin-induced leakage and $1/R_o^2$. For these bilayer systems, k_c should be nearly constant. That is, for some of these lipids (SOPC, DOPC, DOPC/DOPE), k_c has been directly measured (Table 1), and the other systems (8:2 EPC/lysoPC, EPC/DOG) contain lipids with similar hydrocarbon chain compositions to SOPC or DOPC. Although to the best of our knowledge, this is the first demonstration of a quantitative relationship between leakage and spontaneous radius of curvature, several previous investigations have shown that leakage induced by melittin or antimicrobial peptides depends on the shape of the lipid molecule in the bilayer. In the case of melittin, Rex (1996) found a lower leakage for DOPC than for 1-palmitoyl-2-oleoyl-*sn*-glycero-3-phosphocholine and argued that this could be due to the shape of the lipid, as the second double bond makes a larger area per fatty acid chain for DOPC compared to 1-palmitoyl-2-oleoyl-*sn*-glycero-3-phosphocholine. As noted in the Introduction, the addition of lipids with negative curvature decreases peptide-induced leakage, whereas the addition of lipids with positive

curvature increases leakage for magainin (Matsuzaki et al., 1998) and cathelicidin (Basanez et al., 2002). The addition of lysoPC affects the lifetime of gramicidin-A channels (Lundbaek and Andersen, 1994). In the case of alamethicin, spontaneous curvature affects both binding (Lewis and Cafiso, 1999) and conductance states (Keller et al., 1993).

Energetics of bilayer deformations

As detailed in several theoretical treatments (Huang, 1986; Lundbaek et al., 2003; Nielsen et al., 1998), the energy of bilayer deformation (E_{def}) contains several terms. One term, due to effects of bilayer area changes (E_a), is proportional to K_a, and a term due to curvature-elastic effects (E_{curv}) is proportional to k_c/R_o^2. Our observations that the melittin-induced leakage has linear relationships with both K_a (Fig. 3) and $1/R_o^2$ (Fig. 4) indicate that 1) bilayer deformation plays an important role in melittin-induced pore formation and 2) both E_a and E_{curv} are factors in this pore formation. We note one possible reason that the plots of leakage versus K_a and $1/R_o^2$ are not perfectly linear: it is impossible to change one variable (K_a or $1/R_o^2$) without changing the other (Table 1). For example, Fig. 3 shows the effect of systematic changes in K_a on leakage parameters. For most of the systems in this figure, $1/R_o^2$ is approximately the same but does vary for DOPC.

Models for pore formation

The binding and melittin-induced leakage data in this article, as well as other leakage data in the literature, can be explained in terms of pore models, such as the toroidal pore (Ludtke et al., 1996; Matsuzaki et al., 1998; Yang et al., 2001; Zemel et al., 2003), that involve lipid bending and the formation of defects lined, at least in part, by lipid headgroups (Fig. 1 *A*). Specifically, the observed relationships between leakage and K_a (Fig. 3) and $1/R_o^2$ (Fig. 4) are both consistent with the toroidal pore model. Increases in K_a indicate a more cohesive bilayer that is less likely to bend or deform in the presence of melittin. Since toroidal pores involve an invagination of the outer monolayer of the bilayer, pore formation would be favored by the presence of lipids with positive curvature but opposed by lipids with negative curvature (Fig. 1 *B*).

The observed invariance of melittin-induced leakage with differences in bilayer hydrocarbon thickness (Fig. 6) is also evidence in favor of the toroidal pore over the barrel stave pore. In the case of the barrel stave pore, where the peptide penetrates across the bilayer hydrocarbon region (Fig. 1 *A*), one would expect the most stable channel when the length of the peptide transmembrane domain matched the thickness of the bilayer hydrocarbon region. Any ''hydrophobic mismatch'' (Mouritsen and Bloom, 1984) between the length of the transmembrane domain and the bilayer hydrocarbon region would be energetically unfavorable due to the possible exposure of water to nonpolar amino acids or the hydrocarbon region of the bilayer. In the case of the toroidal pore, where the peptide is thought to remain in the lipid headgroup region (Fig. 1 *A*), one would expect the peptide-induced leakage to be not strongly dependent on d_{hc}, as indeed observed with melittin (Fig. 6).

In addition, we argue that the data with PEG-lipids are consistent with a toroidal pore model. As also found by Rex et al. (2002), the incorporation of PEG-lipids has little effect on melittin binding but decreases melittin-induced leakage (Table 1). For the PEG lipid molecular weight and concentration used in these bilayers, theoretical predictions indicate that the PEG-lipid should have little effect on K_a or k_c (Hristova and Needham, 1994), but experimental data show that the PEG chains form a strong steric barrier that extends ~60 Å from the bilayer surface (Kenworthy et al., 1995a). Thus, because of steric hindrance between the attached PEG chains, it would be energetically unfavorable for bilayers containing PEG-lipids to fold into toroidal pores (Fig. 1 *A*), which are thought to have radii considerably smaller than 60 Å (Matsuzaki et al., 1997; Yang et al., 2001). Moreover, even if a pore did form, the PEG chain could plug the aqueous pore, thereby decreasing its permeability.

Data for melittin-induced leakage with chloroplast glycolipids are also consistent with the toroidal pore model. Hincha and Crowe (1996) showed that the incorporation into EPC bilayers of monogalactosyldiglyceride inhibits melittin-induced leakage to a much larger extent than does the incorporation of digalactosyldiglyeride. This could be due to molecular shape and monolayer curvature, as monogalactosyldiglyceride has small headgroup (negative curvature) and forms water filled hexagonal phase by itself, whereas digalactosyldiglyeride, with a larger headgroup, forms bilayers.

The following mechanism for the induction of melittin-induced pores appears to fit the experimental data. First, melittin from the aqueous phase adsorbs to the interfacial region as a monomer and assumes a bent helical conformation (Altenbach et al., 1989; Drake and Hider, 1979). This peptide adsorption expands the outer monolayer relative to the inner monolayer, inducing a bending moment on the bilayer. The monomers dimerize (or aggregate), which may be the rate-limiting step in pore formation (Takei et al., 1999), and create a structural deformation in the membrane. This deformation acts as a nucleation site for other peptides to form a transient pore lined by both peptides and lipid headgroups (Yang et al., 2001). The size of the pore is determined by the charge density of the peptide and the deformation energy of the lipids. Lipids with positive (negative) curvature increase (decrease) permeability by stabilizing (destabilizing) the pore or by increasing (decreasing) the open time probability.

SUMMARY

Changes in bilayer material properties alter both melittin binding and melittin-induced vesicle leakage. For bilayers

with similar melittin binding, we find that melittin-induced leakage depends on the area compressibility modulus, the spontaneous radius of curvature, and the presence of polymer lipids, but is not dependent on the bilayer hydrocarbon thickness. All of these results are supportive of the toroidal model for melittin-induced pore formation.

This work was supported by grants GM27278 and GM584342 from the National Institutes of Health.

REFERENCES

Allende, D., and T. J. McIntosh. 2003. Lipopolysaccharides in bacterial membranes act like cholesterol in eukaryotic plasma membranes in providing protection against melittin-induced bilayer lysis. *Biochemistry.* 42:1101–1108.

Allende, D., A. Vidal, S. A. Simon, and T. J. McIntosh. 2003. Bilayer interfacial properties modulate the binding of amphipathic peptides. *Chem. Phys. Lipids.* 122:65–76.

Altenbach, C., W. Froncisz, J. S. Hyde, and W. L. Hubbell. 1989. Conformation of spin-labeled melittin at membrane surfaces investigated by pulse saturation recovery and continuous wave power saturation electron paramagnetic resonance. *Biophys. J.* 56:1183–1191.

Banemann, A., H. Deppisch, and R. Gross. 1998. The lipopolysaccharide of Bordetella bronchisepticsa acts as a protective shield against antimicrobial peptides. *Infect. Immun.* 66:5607–5612.

Barranger-Mathys, M., and D. S. Cafiso. 1996. Membrane structure of voltage-gated channel forming peptides revealed by site-directed spin labeling. *Biochemistry.* 35:498–505.

Basanez, G., A. E. Shinnar, and J. Zimmerberg. 2002. Interaction of hagfish cathelicidin antimicrobial peptides with model lipid membranes. *FEBS Lett.* 532:115–120.

Ben-Shaul, A., N. Ben-Tal, and B. Honig. 1996. Statistical thermodynamic analysis of peptide and protein insertion into lipid membranes. *Biophys. J.* 71:130–137.

Ben-Tal, N., A. Ben-Shaul, A. Nicolls, and B. Honig. 1996a. Free-energy determinants of alpha-helix insertion into lipid bilayers. *Biophys. J.* 70: 1803–1812.

Ben-Tal, N., B. Honig, R. M. Peitzsch, G. Denisov, and S. McLaughlin. 1996b. Binding of small basic peptides to membranes containing acidic lipids: theoretical models and experimental results. *Biophys. J.* 71:561–575.

Benachir, T., and M. Lafleur. 1995. Study of vesicle leakage induced by melittin. *Biochim. Biophys. Acta.* 1235:452–460.

Benachir, T., M. Monette, J. Grenier, and M. Lafleur. 1997. Melittin-induced leakage from phosphatidylcholine vesicles is modulated by cholesterol: a property used for membrane targetting. *Eur. Biophys. J.* 25:201–210.

Chen, P. S. Jr., T. Y. Toribara, and H. Warner. 1956. Microdetermination of phosphorous. *Anal. Chem.* 28:1756–1758.

Chen, Z., and R. P. Rand. 1997. The influence of cholesterol on phospholipid membrane curvature and bending elasticity. *Biophys. J.* 73: 267–276.

Dan, N., and S. A. Safran. 1998. Effect of lipid characteristics on the structure of transmembrane proteins. *Biophys. J.* 75:1410–1414.

deGennes, P. G. 1987. Polymers at an interface: a simplified view. *Adv. Colloid Interface Sci.* 27:189–209.

Dempsey, C. E. 1990. The actions of melittin on membranes. *Biochim. Biophys. Acta.* 1031:143–161.

Drake, A. F., and R. C. Hider. 1979. The structure of melittin in lipid bilayer membranes. *Biochim. Biophys. Acta.* 555:371–373.

Epand, R. M., and H. J. Vogel. 1999. Diversity of antimicrobial peptides and their mechanisms of action. *Biochim. Biophys. Acta.* 1462:11–28.

Evans, E., and D. Needham. 1987. Physical properties of surfactant bilayer membranes: thermal transitions, elasticity, rigidity, cohesion, and colloidal interactions. *J. Phys. Chem.* 91:4219–4228.

Faucon, J. F., J. Dufourcq, and C. Lussan. 1979. The self-association of melittin and its binding to lipids. An intrinsic fluorescence polarization study. *FEBS Lett.* 102:187–190.

Fuller, N., and R. P. Rand. 2001. The influence of lysolipids on the spontaneous curvature and bending elasticity of phospholipid membranes. *Biophys. J.* 81:243–254.

Gandhavadi, M., D. Allende, A. Vidal, S. A. Simon, and T. J. McIntosh. 2002. Structure, composition, and peptide binding properties of detergent soluble bilayers and detergent resistant rafts. *Biophys. J.* 82:1469–1482.

Gauldie, J., J. M. Hanson, F. D. Rumjanek, R. A. Shipolini, and C. A. Vernon. 1976. The peptide components of bee venum. *Eur. J. Biochem.* 61:369–376.

Hallock, K. J., D. K. Lee, and A. Ramamoorthy. 2003. MSI-78, an analogue of the magainin antimicrobial peptides, disrupts lipid bilayer structure via positive curvature strain. *Biophys. J.* 84:3052–3060.

Henzler Wildman, K. A., D. K. Lee, and A. Ramamoorthy. 2003. Mechanism of lipid bilayer disruption by the human antimicrobial peptide, LL-37. *Biochemistry.* 42:6545–6558.

Hincha, D. K., and J. H. Crowe. 1996. The lytic activity of the bee venom pepide melittin is strongly reduced by the presence of negatively charged phospholipids or chloroplast galactolipids in the membranes of phosphatidylcholine large unilamellar vesicles. *Biochim. Biophys. Acta.* 1284: 162–170.

Hristova, K., and D. Needham. 1994. The influence of polymer-grafted lipids on the physical properties of lipid bilayers: a theoretical study. *J. Colloid Interface Sci.* 168:302–314.

Huang, H. W. 1986. Deformation free energy of bilayer membrane and its effect on gramicidin channel lifetime. *Biophys. J.* 50:1061–1070.

Keller, S. L., S. M. Bezrukov, S. M. Gruner, M. W. Tate, I. Vodyanoy, and V. A. Parsegian. 1993. Probability of alamethicin conductance states varies with nonlamellar tendency of bilayer phospholipids. *Biophys. J.* 65:23–27.

Kenworthy, A. K., K. Hristova, D. Needham, and T. J. McIntosh. 1995a. Range and magnitude of the steric pressure between bilayers containing phospholipids with covalently attached poly(ethyleneglycol). *Biophys. J.* 68:1921–1936.

Kenworthy, A. K., S. A. Simon, and T. J. McIntosh. 1995b. Structure and phase behavior of lipid suspensions containing phospholipids with covalently attached poly(ethylene glycol). *Biophys. J.* 68:1903–1920.

Kessel, A., and N. Ben-Tal. 2002. Free energy determinants of peptide association with lipid bilayers. *In* Peptide-Lipid Interaction. S. A. Simon and T. J. McIntosh, editors. San Diego, Academic Press. *Curr. Top. Membr.* 52:205–253.

Kessel, A., D. S. Cafiso, and N. Ben-Tal. 2000. Continuum solvent model calculations of alamethicin-membrane interactions: thermodynamic aspects. *Biophys. J.* 78:571–583.

Ladokhin, A. S., M. E. Selsted, and S. H. White. 1997a. Sizing membrane pores in lipid vesicles by leakage of co-encapsulated markers: pore formation by melittin. *Biophys. J.* 72:1762–1766.

Ladokhin, A. S., M. E. Selsted, and S. H. White. 1997b. Bilayer interactions of indolicidin, a small antimicrobial peptide rich in tryptophan, prolien, and basic amino acids. *Biophys. J.* 72:794–805.

Ladokhin, A. S., and S. H. White. 2001. 'Detergent-like' permeabilization of anionic lipid vesicles by melittin. *Biochim. Biophys. Acta.* 1514:253–260.

Leikin, S., M. M. Kozlov, N. L. Fuller, and R. P. Rand. 1996. Measured effects of diacylglycerol on structural and elastic properties of phosholipid membranes. *Biophys. J.* 71:2623–2632.

Lewis, J. R., and D. S. Cafiso. 1999. Correlation of the free energy of a channel-forming voltage-gated peptide and the spontaneous curvature of bilayer lipids. *Biochemistry.* 38:5932–5938.

Ludtke, S. J., K. He, W. T. Heller, T. A. Harroun, L. Yang, and H. W. Huang. 1996. Membrane pores induced by magainin. *Biochemistry.* 35:13723–13728.

Lundbaek, J. A., and O. S. Andersen. 1994. Lysophospholipids modulate channel function by altering the mechanical properties of lipid bilayers. *J. Gen. Physiol.* 104:645–673.

Lundbaek, J. A., O. S. Andersen, T. Werge, and C. Nielsen. 2003. Cholesterol-Induced protein sorting: an analysis of energetic feasibility. *Biophys. J.* 84:2080–2089.

Lundbaek, J. A., P. Birn, A. J. Hansen, R. Sogaard, C. Nielsen, J. Girshman, M. J. Bruno, S. E. Tape, J. Egebjerg, D. V. Greathouse, G. L. Mattice, R. E. Koeppe 2nd, and others. 2004. Regulation of sodium channel function by bilayer elasticity: the importance of hydrophobic coupling. effects of micelle-forming amphiphiles and cholesterol. *J. Gen. Physiol.* 123:599–621.

Maingret, F., A. J. Patel, F. Lesage, M. Lazdunski, and E. Honore. 2000. Lysophospholipids open the two-pore domain mechano-gated K(+) channels TREK-1 and TRAAK. *J. Biol. Chem.* 275:10128–10133.

Matsuzaki, K., O. Murase, N. Fujii, and K. Miyajima. 1996. An antimicrobial peptide, magainin 2, induced rapid flip-flop of phopsholipids coupled wih pore formation and peptide translocation. *Biochemistry.* 35:11361–11368.

Matsuzaki, K., K. Sugishita, N. Ishibe, M. Ueha, S. Nakata, K. Miyajima, and R. M. Epand. 1998. Relationship of membrane curvature to the formation of pores by magainin 2. *Biochemistry.* 37:11856–11863.

Matsuzaki, K., S. Yoneyama, and K. Miyajima. 1997. Pore formation and translocation of melittin. *Biophys. J.* 73:831–838.

May, S., and A. Ben-Shaul. 1999. Molecular theory of lipid-protein interaction and the Lalpha-HII transition. *Biophys. J.* 76:751–767.

McIntosh, T. J., S. Advani, R. E. Burton, D. V. Zhelev, D. Needham, and S. A. Simon. 1995. Experimental tests for protrusion and undulation pressures in phospholipid bilayers. *Biochemistry.* 34:8520–8532.

McIntosh, T. J., and P. W. Holloway. 1987. Determination of the depth of bromine atoms in bilayers formed from bromolipid probes. *Biochemistry.* 26:1783–1788.

McIntosh, T. J., A. D. Magid, and S. A. Simon. 1987. Steric repulsion between phosphatidylcholine bilayers. *Biochemistry.* 26:7325–7332.

McIntosh, T. J., A. D. Magid, and S. A. Simon. 1989. Cholesterol modifies the short-range repulsive interactions between phosphatidylcholine membranes. *Biochemistry.* 28:17–25.

McIntosh, T. J., and S. A. Simon. 1986. The hydration force and bilayer deformation: a reevaluation. *Biochemistry.* 25:4058–4066.

Mouritsen, O. G., and M. Bloom. 1984. Mattress model of lipid-protein interactions in membranes. *Biophys. J.* 46:141–153.

Needham, D. (1995). Cohesion and permeability of lipid bilayer vesicles. *In* Permeability and Stability of Lipid Bilayers. E. A. Disalvo and S. A. Simon, editors. CRC Press, Boca Raton, FL. 49–76.

Needham, D., and R. S. Nunn. 1990. Elastic deformation and failure of lipid bilayer membranes containing cholesterol. *Biophys. J.* 58:997–1009.

Nielsen, C., and O. S. Andersen. 2000. Inclusion-induced bilayer deformations: effects of monolayer equilibrium curvature. *Biophys. J.* 79: 2583–2604.

Nielsen, C., M. Goulian, and O. S. Andersen. 1998. Energetics of inclusion-induced bilayer deformations. *Biophys. J.* 74:1966–1983.

Oliver, D., C. C. Lien, M. Soom, T. Baukrowitz, P. Jonas, and B. Fakler. 2004. Functional conversion between A-type and delayed rectifier K+ channels by membrane lipids. *Science.* 304:265–270.

Patel, A. J., M. Lazdunski, and E. Honore. 2001. Lipid and mechano-gated 2P domain K(+) channels. *Curr. Opin. Cell Biol.* 13:422–428.

Pawlak, M., S. Stankowski, and G. Schwarz. 1991. Melittin induced voltage-dependent conductance in DOPC lipid bilayers. *Biochim. Biophys. Acta.* 1062:94–102.

Quay, S. C., and C. C. Condie. 1983. Conformational studies of aqueous melittin: thermodynamic parameters of monomer-tetramer self-assocation reaction. *Biochemistry.* 22:695–700.

Rand, R. P., N. L. Fuller, S. M. Gruner, and V. A. Parsegian. 1990. Membrane curvature, lipid segregation, and structural transitions for phospholipids under dual-solvent stress. *Biochemistry.* 29:76–87.

Rawicz, W., K. C. Olbrich, T. McIntosh, D. Needham, and E. Evans. 2000. Effect of chain length and unsaturation on elasticity of lipid bilayers. *Biophys. J.* 79:328–339.

Rex, S. 1996. Pore formation induced by the peptide melittin in different lipid vesicle membranes. *Biophys. Chem.* 58:75–85.

Rex, S., J. Bian, J. Silvius, and M. Lafleur. 2002. The presence of PEG-lipids in liposomes does not reduce melittin binding but decreases melittin-induced leakage. *Biochim. Biophys. Acta.* 1558:211–221.

Rex, S., and G. Schwarz. 1998. Quantitative studies on the melittin-induced leakage mechanism of lipid vesicles. *Biochemistry.* 37:2336–2345.

Sophianopoulos, J. A., S. J. Durham, A. J. Sophianopoulos, H. L. Ragsdale, and W. P. Cropper. 1978. Ultrafiltration is theoretically equivalent to equilibrium dialysis but much simpler to carry out. *Arch. Biochem. Biophys.* 187:132–137.

Stankowski, S., M. Pawlak, E. Kaisheva, C. H. Robert, and G. Schwarz. 1991. A combined study of aggregation, membrane affinity and pore activity of natural and modified melittin. *Biochim. Biophys. Acta.* 1069: 77–86.

Szule, J. A., N. L. Fuller, and R. P. Rand. 2002. The effects of acyl chain length and saturation of diacylglycerols and phosphatidylcholines on membrane monolayer curvature. *Biophys. J.* 83:977–984.

Takei, J., A. Remenyi, and C. E. Dempsey. 1999. Generalised bilayer perturbation from peptide helix dimerisation at membrane surfaces: vesicle lysis induced by disulphide-dimerised melittin analogues. *FEBS Lett.* 442:11–14.

Tosteson, M. Y., and D. C. Tosteson. 1981. The sting: melittin forms channels in lipid bilayers. *Biophys. J.* 36:109–116.

Voglino, L., T. J. McIntosh, and S. A. Simon. 1998. Modulation of the binding of signal peptides to lipid bilayers by dipoles near the hydrocarbon-water interface. *Biochemistry.* 37:12241–12252.

Voglino, L., S. A. Simon, and T. J. McIntosh. 1999. Orientation of LamB signal peptides in bilayers: influence of lipid probes on peptide binding and interpretation of fluorescence quenching data. *Biochemistry.* 38: 7509–7516.

White, S. H., and W. C. Wimley. 1999. Membrane protein folding and stability: physical principles. *Annu. Rev. Biophys. Biomol. Struct.* 28: 319–365.

Yang, L., T. A. Harroun, T. M. Weiss, L. Ding, and H. W. Huang. 2001. Barrel-stave model or toroidal model? A case study on melittin pores. *Biophys. J.* 81:1475–1485.

Yang, L., T. M. Weiss, R. I. Lehrer, and H. W. Huang. 2000. Crystallization of antimicrobial pores in membranes: magainin and protegrin. *Biophys. J.* 79:2002–2009.

Zemel, A., D. R. Fattal, and A. Ben-Shaul. 2003. Energetics and self-assembly of amphipathic peptide pores in lipid membranes. *Biophys. J.* 84:2242–2255.

Zhelev, D. 1998. Material property characteristics for lipid bilayers containing lysolipids. *Biophys. J.* 75:321–330.